Evaluation of AW3D30 Elevation Accuracy in China

Fan Mo[1], Junfeng Xie[1] and Yuxuan Liu[2]
[1]*Satellite Surveying and Mapping Application Center, NASG, Beijing, China*
[2]*School of Remote Sensing and Information Engineering, University of Wuhan, Wuhan, China*

Keywords: Digital Surface Model, AW3D30, ALOS DSM, Elevation Accuracy Evaluation, National Control Point Image Database.

Abstract: The AW3D30 dataset is a publically available, high-accuracy digital surface model; the model's cited nominal elevation accuracy is 5 m (1σ). In order to verify the accuracy of AW3D30, we selected China as test area, and used field measurement points in the national control point image database as control data. The elevation accuracy of the field measurement points in the national control point image database is better than 1 m. The results show that the accuracy of the AW3D30 satisfies the requirement of 5 m nominal accuracy, and elevation accuracy reached 2 m (1σ). Accuracy is related to both terrain and slope. Accuracy is better in flat areas than in areas of complex terrain, and the eastern region of China is characterized by better accuracy than the western region.

1 INTRODUCTION

The Advanced Land Observing Satellite (ALOS) is a high-resolution three-line array stereo remote sensing surveying satellite launched by Japan Aerospace Exploration Agency (JAXA) on January 24, 2006. Its primary mission is to complete global key area 1:25000 scale terrain mapping (Rosenqvist et al., 2007; Shimada et al., 2010). The Panchromatic Remote-sensing Instrument for Stereo Mapping (PRISM) carried by ALOS has three 2.5-meter resolution panchromatic cameras that are used for front view, nadir view and rear view of earth observation along the track direction, respectively. Precise three-dimensional surface information can be obtained through front intersection processing (Takaku and Tadono, 2009; Rosenqvist et al., 2014).

On May 31, 2016, JAXA released the ALOS Global Digital Surface Model "ALOS World 3D-30 m" (AW3D30). The model produced a global 30-meter grid using ALOS stereoscopic images with elevation nominal accuracy of 5 meters. The AW3D30 currently possesses the highest accuracy among global public digital elevation models. The accuracy has been verified in many countries around the world (Zhihua et al., 2017; Takaku et al., 2014; Tadono et al., 2014).

In order to verify the accuracy of AW3D30 elevation data in China, we adopted the national control point image database as an evaluation benchmark. This image database is a core component of the Environment and Disaster Monitoring Engineering Based on Moonlet Constellation. The database contains a total of about 350,000 generalized control points, including about 73,000 field measurement control points. The initial aim of this database is to meet the need of matching with satellite optical images. The overall accuracy of the control point image database can meet plane and elevation requirements of national 1:50,000 scale mapping (Yu, 2012). The elevation accuracy of the field measurement control points acquired by GPS-RTK (Global Position System Real Time Kinematic) included in the database is better than 1 m. Therefore, by using the control point image database as a control benchmark, we can precisely and objectively evaluate the elevation accuracy of AW3D30 data in China.

2 DATA DESCRIPTION

2.1 AW3D30

ALOS had been running on track for 5 years, acquiring a large number of image data with global coverage. AW3D30 data were generated from approximately 3 million ALOS PRISM 2.5 m

Mo, F., Xie, J. and Liu, Y.
Evaluation of AW3D30 Elevation Accuracy in China.
DOI: 10.5220/0006674401800186
In *Proceedings of the 4th International Conference on Geographical Information Systems Theory, Applications and Management (GISTAM 2018)*, pages 180-186
ISBN: 978-989-758-294-3

resolution three-line array stereo imaging that, in general, covered global land areas. Due to the limitations of panchromatic camera imaging, there are few images for global waters. Thus, the AW3D30 data do not include information on ocean elevations.

The original digital surface model (DSM) data from AW3D30 are 5-meter grid digital images. However, because of the amount of data generated (and other reasons), JAXA only publicly released the 30 meter grid AW3D30 data. The released AW3D30 data contain two versions related to differences in the 5 to 30 meter down-sample processing: AVE and MED. AVE uses a mean filter to down-sample the raw data, whereas MED uses a median filter.

According to JAXA's release plan, AW3D30 data are divided into three versions. Currently released AW3D30 data belong to the version 1.1; the main date parameters associated with this version are shown in Table 1 (Takaku et al., 2016; Tadono et al., 2016).

Table 1: Listing of the primary parameters of the AW3D30.

Parameter l	Value
Image file	16-bit integer, gray value represents elevation, the unit is meter
Each view coverage area	1° × 1°
Resolution	1" × 1"
Vertical accuracy	5 m (RMSE)
Coordinate system	Latitude and longitude (ITRF97 [GRS80])
Elevation type	Normal

Since the elevation type of AW3D30 data are normal height, it is necessary to introduce an geoid height when performing an elevation accuracy evaluation. In order to control the data on the same elevation reference, we used the EGM2008 model to calculate the geoid height of corresponding points (Pavlis et al., 2013; Hirt et al., 2011).

2.2 Control Point Image Database

China covers a vast area characterized by large climatic difference between the North and the South. Due to its size, disasters are difficult to monitor in real time, resulting in a greater threat to public's safety and economic security. For this reason, the Ministry of Civil Affairs National Disaster Reduction Center started the national control point image database construction project in 2010. The project took the China Institute of Surveying and Mapping two years to complete. The control point image database covers a total of 31 provinces (Taiwan, Hong Kong and Macau are not covered).
The control point image database contains about 350,000 generalized control points, most of which are pass points, as well as some field measurement points and measurement points obtained from large-scale aeronautical digital orthography model (DOM). The accuracy of the pass points and the large-scale aeronautical DOM image internal collection points is lower than that of field acquisition measurement points. Therefore, only the field acquisition measurement points in the control point image database were selected as experimental control data. During the process of evaluating elevation accuracy of the DSM, there is no need to measure an image point; hence, there is no measurement error in this process. The accuracy of the selected elevation control data is better than 1 m (Yu, 2012).

3 RESEARCH METHOD

3.1 Nationwide Comprehensive Evaluation

At present, AW3D30 data cover all global lands, including the entire territory of China. In order to macroscopically verify the overall accuracy of the AW3D30 elevation data in China, we selected all the field measurement points in the national control point image database to evaluate the elevation accuracy of AW3D30 data in the coverage area. Then, we individually calculated each province as an independent sample to examine trends in the accuracy of the nationwide AW3D30 data based on a provincial division.

3.2 Typical Terrain Evaluation

China is vast, extending from a longitude of E73°33' to E135°05' and latitude of N3°51' to N53°33'. In general, China's terrain is elevated in the west and low in the east, and exhibits a ladder-like distribution. The mainland of China is topographically complex, and can be subdivided into five basic types of terrain: plateaus, mountains, plains, hills and basins. The basic terrain types in mainland China are shown in Table 2.

Given the imaging mechanism of ALOS PRISM sensors, different terrain may exhibit different mapping accuracy. Therefore, in order to validate the elevation accuracy of AW3D30 data under different terrain conditions, we selected typical areas within the five terrain types for accuracy analysis, and quantitatively evaluated the elevation accuracy of AW3D30 data within each type of terrain.

Table 2: Basic types of terrain (landscapes) in China.

Terrain	Elevation variations	Typical areas
Plateau	Elevation >1000 meters, with gentle hills	Qinghai-Tibet Plateau, Inner Mongolia Plateau, Loess Plateau, Yunnan-Guizhou Plateau and Pamirs
Mountain	Elevation >500 meters, with large topographic variations	Great Himalayas, Hengduan Mountains, Nanling, Qinling and Taihang Mountains
Plain	Elevation of <200 meters, relatively flat terrain	Northeast plain, North China Plain, middle and lower of Yangtze River, and Ganges River Plain
Hill	Relative height <200 meters, with gentle variation in topography	Jiangnan hills and Shandong hills
Basin	Depression characterized by low areas in the middle, high areas on both sides	Tarim Basin, Junggar Basin, Qaidam Basin, Sichuan Basin and Turpan Basin

3.3 Evaluation based on Terrain Slope

The base-height ratio of a space-borne optics stereo camera is generally small compared with aerial photogrammetry. As a result, on-orbit imaging is greatly affected by the terrain. In areas with large topographic variations, the accuracy of stereoscopic plotting is often poor; therefore, accuracy of the AW3D30 in topographically complex areas needs to be examined under different slope conditions (Hodgson, 2005). The slope of the terrain was calculated using the following expression (Zhihua et al., 2017):

$$S = \arctan\left(\frac{(z_2 - z_1)^2}{(x_2 - x_1)^2 + (y_2 - y_1)^2}\right) \quad (1)$$

where (x_1, y_1, z_1) and (x_2, y_2, z_2) indicate the two-point three-dimensional coordinate values along the slope to be calculated.

3.4 Evaluation Method

We selected the field measurement control points in the national control point image database as control data for the accuracy evaluation. We directly used coordinates information (X,Y,Z) in the database as an evaluation benchmark, rather than the control point image. Specifically, values of (X,Y) were substituted into the AW3D30 data. These data can be interpolated to get corresponding elevation information. Bilinear interpolation method is applied (Qinghua et al., 2010; Arun, 2013). As shown in figure 1, the point $Z'(X,Y)$ can be calculated from four vertex values of its grid $P_{i,j}$, $P_{i+1,j}$, $P_{i,j+1}$ and $P_{i+1,j+1}$. The formula used in the calculation was:

$$\begin{aligned} Z'(X,Y) &= (1-\Delta x)(1-\Delta y)P_{i,j} + \\ &\Delta x(1-\Delta y)P_{i+1,j} + (1-\Delta x)\Delta y P_{i,j+1} + \Delta x \Delta y P_{i+1,j+1} \end{aligned} \quad (2)$$

where Δx and Δy are the coordinate increments of point A relative to point $P_{i,j}$ when the grid side length is 1.

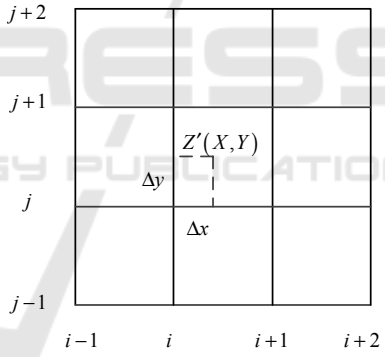

Figure 1: Diagram illustrating how bilinear interpolation was defined.

By using this interpolation method, we were able to obtain the elevation information Z' that corresponds to the point. Invalid points were identified by the mask image among the AW3D30 auxiliary data, and gross errors in elevation differences (where a point with an absolute difference value between Z' and Z greater than 100 m is defined as a gross error) were eliminated. Finally, we analyzed the accuracy of the AW3D30 in different confidence intervals. The elevation accuracy parameters mainly include the mean value, absolute mean value, standard deviation and root mean square error of the difference between Z' and Z (Athmania and Achour, 2014). The specific formulas are as follows:

The mean of the difference:

$$V_{mean} = \frac{\sum(Z_i' - Z_i)}{n} \quad (3)$$

Absolute mean value of the difference:

$$V_{abs} = \frac{\sum|Z_i' - Z_i|}{n} \quad (4)$$

Standard deviation:

$$V_{std} = \sqrt{\frac{\sum(Z_i' - Z_i - V_{mean})^2}{n}} \quad (5)$$

Root mean square error:

$$V_{RMSE} = \sqrt{\frac{\sum(Z_i' - Z_i)^2}{n}} \quad (6)$$

4 EXPERIMENT AND ANALYSIS

All field acquisition measurement points in the control point image database were selected for analysis, resulting in a total of about 73,000 points. They were even distributed in China. These points were substituted into the AW3D30 for obtaining elevation information. The pixel value obtained was the elevation value of the point. The difference between the elevation value obtained and value of the corresponding control point was then calculated to analyze the elevation accuracy. Moreover, differences between the histograms constructed for the AVE and MED data are sustainable. A histogram of elevation differences about AVE is shown in Figure 2.

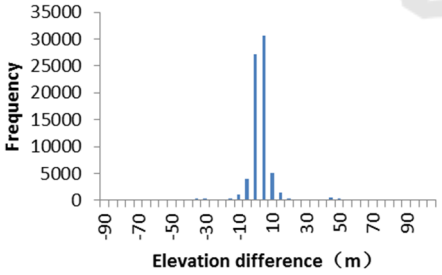

Figure 2: Histograms of elevation difference.

Elevation difference calculated as the elevation of the control point minus the corresponding elevation contained in the AW3D30 dataset. Figure 2 shows that the elevation differences are normally distributed, and mainly concentrated around 0. Using all of the control points as benchmarks, we calculated the mean, absolute mean value, standard deviation and root mean square error of corresponding AW3D30. The overall accuracy determined for the entire country is shown in Table 3.

Table 3: Nationwide elevation accuracy in China.

Criteria	Parameter	Value	
		AVE (m)	MED (m)
1σ	Mean	0.2	0.13
	Absolute mean	1.47	1.46
	Standard deviation	1.73	1.73
	RMSE	1.74	1.73
2σ	Mean	0.36	0.33
	Absolute mean	3.11	4.57
	Standard deviation	4.44	4.41
	RMSE	4.46	4.42
3σ	Mean	0.79	0.75
	Absolute mean	4.6	4.57
	Standard deviation	9.11	9.09
	RMSE	9.15	9.15

Accuracy of AW3D30 data in China fall within an elevation accuracy of 5 m (1σ), locally reaching 2 m (1σ). With regards to the 2σ confidence interval, the elevation accuracy reaches 5 m; in the 3σ confidence interval, elevation accuracy reaches 10 m. As presented in Table 3, accuracy of the AVE and MED data is similar.

In order to evaluate whether the accuracy of the AW3D30 are related to the terrain, province was selected as a unit of study. The root mean square error of MED and control point data for each province, along with trends obtained on the overall accuracy are shown in figure 3 In general, accuracy of the AW3D30 elevation date in the eastern region is better than that in the western region, while accuracy in the northern region is slightly better than that in the southern region. Areas of high elevation accuracy are mainly concentrated in two regions: Inner Mongolia-northeast China and north China. Tibet has the lowest accuracy in elevation, followed by the regions of Yunnan-Sichuan-Qinghai-Xinjiang.

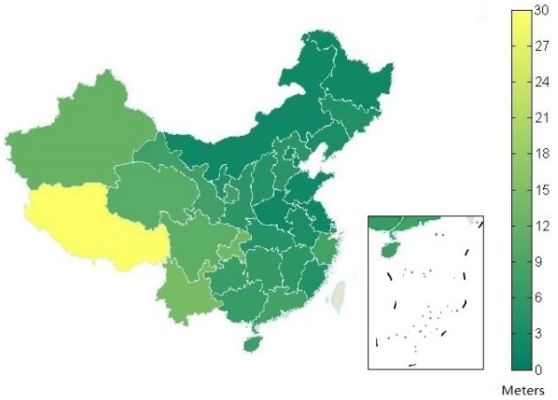

Figure 3: Geographical patterns in accuracy of AW3D30 data.

In order to understand the impact of different terrain types on the accuracy of the AW3D30 data, we analyzed the accuracy associated with each of the five delineated terrains in China (Table 2). Large sections representative of the typical terrain were used as experimental areas. We selected two experimental areas in every typical terrain, and these areas are different in landform. The field measurement points in the control point image database from these areas were used to calculate elevation accuracy parameters between the control point and AW3D30. Points with gross errors were removed. The obtained elevation accuracy within the 3σ confidence interval was then determined (Table 4).

Table 4: Accuracy in AW3D30 stratified by terrain type.

Terrain	Name	Parameter	Value (m)	
			AVE	MED
Plateau	Qinghai-Tibet Plateau	Mean	−11.93	−11.89
		Absolute mean value	20.14	20.08
		Standard deviation	22.96	22.87
		RMSE	25.87	25.77
	Inner Mongolia Plateau	Mean	−3.04	−3.08
		Absolute mean value	3.28	3.32
		Standard deviation	2.44	2.43
		RMSE	3.9	3.94
Mountain	Hengduan Mountains	Mean	−3.4	−3.4
		Absolute mean value	10.08	10.04
		Standard deviation	17.24	17.25
		RMSE	17.58	17.58
	Taihang Mountains	Mean	−2.57	−2.6
		Absolute mean value	6.26	6.26
		Standard deviation	11.54	11.54
		RMSE	11.82	11.82
Plain	Northeast Plain	Mean	0	−0.03
		Absolute mean value	1.84	1.84
		Standard deviation	2.54	2.53
		RMSE	2.55	2.53
	North China Plain	Mean	1.86	1.82
		Absolute mean value	2.46	2.41
		Standard deviation	2.45	2.42
		RMSE	3.07	3.03
Hills	Jiangnan Hills	Mean	0.1	−0.03
		Absolute mean value	3.48	3.33
		Standard deviation	4.63	4.72
		RMSE	4.64	4.72
	Shandong Hills	Mean	−2.91	−2.92
		Absolute mean value	3.26	3.26
		Standard deviation	2.98	3.02
		RMSE	4.17	4.21
Basin	Junggar Basin	Mean	−3.67	−3.69
		Absolute mean value	3.68	3.68
		Standard deviation	3.44	3.45
		RMSE	4.4	4.42
	Qaidam Basin	Mean	3.54	3.57
		Absolute mean value	3.8	3.79
		Standard deviation	4.42	4.41
		RMSE	4.56	4.56

Table 4 shows that the AW3D30 data coverage in the plateaus and mountains are significantly worse than in areas of plains, hills and basins (of which the Inner Mongolia Plateau is highly precise, primarily because the landscape consists of plateaus and the terrain is flat). Elevation accuracy of the AW3D30 covering plateaus is not as good as for the mountains. The plains have the best elevation accuracy, followed by hills and basins. The accuracy of MED is slightly better than that of AVE, especially in the case of flat terrain.

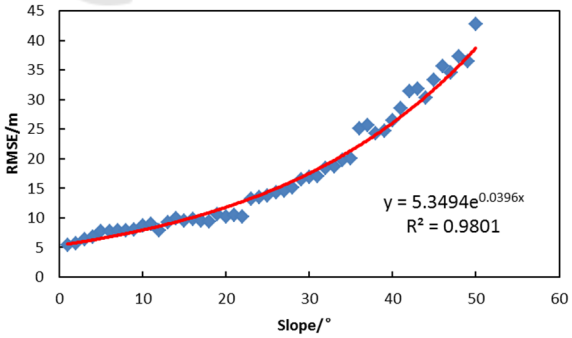

Figure 4: Variation in root mean square error versus slope.

Figure 4 suggests that accuracy is a function of slope, the elevation accuracy of AW3D30 is different in different terrain slopes. In order to analyze the specific impact, AVE AW3D30 data

were examined as an example by sorting the national control points into different slope categories. The slope was calculated by four values in AW3D30 around the control point in the database; specifically, two points before and after the control point in the x direction and two points before and after the control point in the y direction. The sorting slope interval is 1°. We then calculated the corresponding root mean square error in each slope category, plotted the root mean square error value of the elevation according to slope variation, and used the exponential curve for fitting. Figure 4 shows that there is a strong statistically significant (R^2 = 0.9801) positive correlation between the elevation root mean square error and the slope in the AW3D30.

5 CONCLUSIONS

Approximately 73,000 highly precise field measurement points contained in the control point image database were used as elevation reference data. Accuracy of AW3D30 were analyzed at two different spatial scales, all of which showed that AW3D30 satisfies the nominal accuracy of 5 m (1σ) elevation. In general, the elevation accuracy of AW3D30 in China can reach 2 m (1σ), while most of AW3D30 exhibit an accuracy of better than 10 m (3σ). Moreover, an analysis of plateaus, mountains and other areas characterized by large topographic variations exhibited relatively poor accuracy. The accuracy of AW3D30 data for hills, basins, plains and other area with subdued topographic variations was better. The results of the provincial analysis show that the accuracy of the AW3D30 data gradually declines from the eastern region to the western region. Similarly, accuracy gradually decreases from the northern region to the southern region. The accuracy of AW3D30 also has a strong correlation to slope. The results obtained in this analysis demonstrate that the accuracy of AW3D30 in China can be effectively used in subsequent scientific studies or engineering practices.

ACKNOWLEDGEMENTS

This work was supported by the Natural Science Foundation of China (No. 41301525, No. 41571440 and No. 41771360), the High Resolution Remote Sensing, surveying and mapping Application Demonstration System Research Program (Issue No. 1), the NASG Young Academic Leaders Foundation (No. 201607), National key research and development program (No. 2017YFB0504201), and the Authenticity Validation Technology of Elevation Measurement Accuracy of GF-7 Laser Altimeter (No. 42-Y20A11-9001-17/18).

REFERENCES

Arun, P., 2013. A comparative analysis of different DEM interpolation methods. *The Egyptian Journal of Remote Sensing and Space Sciences,* 16: 133-139.

Athmania, D., Achour, H., 2014. External Validation of the ASTER GDEM2, GMTED2010 and CGIAR-CSI-SRTM v4.1 Free Access Digital Elevation Models (DEMs) in Tunisia and Algeria. *Remote Sensing*, 6: 4600-4620.

Hirt, C., Gruber, T., Featherstone, W., 2011. Evaluation of the first GOCE static gravity field models using terrestrial gravity, vertical deflections and EGM2008 quasigeoid heights. *Journal of Geodesy*, 85: 723-740.

Hodgson, M., 2005. An Evaluation of Lidar-derived Elevation and Terrain Slope in Leaf-off Conditions. *Photogrammetric Engineering and Remote Sensing*, 71: 817-824.

Pavlis, N., Holmes, S., Kenyon, S., et al., 2013. Correction to 'The Development and Evaluation of the Earth Gravitational Model 2008 (EGM2008)'. *Journal of Geophysical Research*, 118: 2633-2633.

Qinghua, G., Wenkai, L., Hong, Y., et al., 2010. Effects of Topographic Variability and Lidar Sampling Density on Several DEM Interpolation Methods. *Photogrammetric Engineering and Remote Sensing*, 76: 701-712.

Rosenqvist, A., Shimada, M., Suzuki, S., et al., 2014. Operational performance of the ALOS global systematic acquisition strategy and observation plans for ALOS-2 PALSAR-2. *Remote Sensing of Environment*, 155: 3-12.

Rosenqvist, A., Shimada, M., Ito, N., et al., 2007. ALOS PALSAR: A Pathfinder Mission for Global-scale Monitoring of the Environment, *IEEE Transactions on Geoscience and Remote Sensing*, 45: 3307-3316.

Shimada, M., Tadono, T., Rosenqvist, A., 2010. Advanced Land Observing Satellite (ALOS) and Monitoring Global Environmental Change. *Proceedings of the IEEE*, 98: 780-799.

Tadono, T., Ishida, H., Oda, F., et al., 2014. Precise Global DEM Generation by ALOS PRISM. *ISPRS Annals of the Photogrammetry. Remote Sensing Spatial Information Science*, II-4: 71-76.

Tadono, T., Nagai, H., Ishida, H., Iwamoto, H., et al., 2016. Initial Validation of the 30 m-mesh Global Digital Surface Model Generated by ALOS PRISM. *The International Archives of the Photogrammetry, Remote Sensing and Spatial Information Sciences, ISPRS*, XLI-B4: 157-162.

Takaku J., Tadono, T., 2009. PRISM On-Orbit Geometric Calibration and DSM Performance. *IEEE Transcation on Geoscience and Remote Sensing*, 47: 4060-4073.

Takaku, J., Tadono, T., Tsutsui, K., 2014. Generation of High Resolution Global DSM from ALOS PRISM. In *Proceedings of the International Archives of the Photogrammetry, Remote Sensing and Spatial Information Sciences. ISPRS TC IV Symposium*, XL-4: 243–248.

Takaku, J., Tadono, T., Tsutsui, K., et al., 2016. Validation of 'AW3D' Global DSM Generated from ALOS PRISM. *The International Archives of the Photogrammetry, Remote Sensing and Spatial Information Sciences*, III-4: 25-31.

Yu, W., 2012. *Geometry Processing Service Based on Ground Control Point Image Database*. Master's thesis, Shandong University of Science and technology, Tsingtao.

Zhihua, H., Jianwei, P., Yaolin, H., 2017. Evaluation of Recently Released Open Global Digital Elevation Models of Hubei, China. *Remote Sensing*, 9: 262.